The computation of electron transfer rates: The nonadiabatic instanton solution

Jianshu Cao, Camilla Minichino,[a] and Gregory A. Voth
Department of Chemistry, University of Pennsylvania, Philadelphia, Pennsylvania 19104-6323

(Received 3 January 1995; accepted 17 April 1995)

A computational theory for determining electron transfer rate constants is formulated based on an instanton expression for the quantum rate and the self-consistent solution of the imaginary time nonadiabatic steepest descent approximation. The theory obtains the correct asymptotic behavior for the electron transfer rate constant in the nonadiabatic and adiabatic cases, and it smoothly bridges between those two limits for intermediate couplings. Furthermore, no assumptions regarding the form of the diabatic potentials are invoked (e.g., harmonic) and more than two diabatic states can be included in the calculations. The method thereby holds considerable promise for computing electron transfer rate constants in realistic condensed phase systems. © *1995 American Institute of Physics.*

I. INTRODUCTION

Electron transfer (ET) processes in chemistry, physics, and biology have been the subject of a considerable number of experimental and theoretical studies.[1,2] Recent computational approaches for computing ET rate constants range from those based on Fermi's golden rule[3] to explicit quantum dynamical calculations on simplified models of ET processes.[4–9] In addition, approaches derived from path integral quantum transition state theory[10–13] have been developed to calculate the ET rate based on the centroid density of the electronic state variable.[14–16] Despite the many theoretical and computational studies of ET reactions, a unified computational approach has not yet been developed which is capable of determining ET rate constants for arbitrary values of the electronic coupling in systems characterized by general nonlinear potentials and/or a significant degree of nuclear mode tunneling. Significant progress towards this goal will be described in the present paper.

The underlying basis of the theory described herein is the semiclassical approximation to the quantum partition function,[17] which can be shown to be closely related to the thermally averaged quantum tunneling rate in metastable systems.[18–21] Along these lines, Miller has suggested that the quantum reactive flux at low temperature can be determined by the so-called bounce trajectory on the inverted potential energy surface, i.e., the instanton.[19] In terms of the steepest descent approximation, the instanton trajectory along the periodic imaginary time axis satisfies the Euler–Lagrange equation, and the quantum fluctuations along the trajectory take the form of a Gaussian functional which can be calculated by evaluating the Van Vleck determinant.[22] The extension of these ideas to the dissipative quantum tunneling regime has been discussed by Caldeira and Leggett at some length.[23] However, while the original instanton analysis is suitable when a unique potential energy surface can be assumed, an effort to include the possibility of nonadiabatic transitions to other potential surfaces is necessary in order to correctly describe electron transfer processes in a general way. This is the focus of the present analysis.

Many advances have taken place in the field of nonadiabatic dynamics simulation for real time quantum dynamics (see, e.g., Refs. 24–27). The theoretical basis for several algorithms[24,27] is the Pechukas theory of nonadiabatic collisions.[28,29] Although it was originally formulated for real time quantum dynamics, the self-consistent nonadiabatic theory of Pechukas bears a similarity to the instanton theory, both being based on the stationary phase (or steepest descent) approximation to a Feynman path integral.[30,31] The former theory is a real time formulation, while the latter is in imaginary time. In the present paper, the nonadiabatic theory of Pechukas will be combined with the instanton theory to yield a novel and computationally powerful approach for the calculation of electron transfer rate constants under rather general conditions.

The present paper is organized as follows: In Sec. II, the basic ''nonadiabatic instanton'' approach is formulated. A numerical algorithm for solving the equations is then detailed in Sec. III, and results are presented for some representative examples. Concluding remarks are given in Sec. IV.

II. GENERAL FORMALISM

To put the formalism in the most general context, we consider the Hamiltonian for a many-body, multilevel system, given by

$$H = H_d(\mathbf{q}) + H_b(\mathbf{r}) + V_{\rm int}(\mathbf{q},\mathbf{r}), \tag{2.1}$$

where $\mathbf{q}$ is the collection of N nuclear degrees of freedom of an electron transfer system of interest, $\mathbf{r}$ is the collection of the ''bath'' nuclear degrees of freedom, H_d is the part of Hamiltonian defined on an electronically diabatic basis, H_b is the bath Hamiltonian, and $V_{\rm int}$ is the interaction potential between the system and the bath. The Hamiltonian H_d can be

[a]Permanent address: Dipartimento di Chimica, Universitá della Basilicata, Via Nazario Sauro 85, I-85100, Potenza, Italy.

explicitly expressed in terms of the elements h_{ii} (for the ith diabatic surface) and h_{ij} (for the coupling between the ith and jth diabatic surfaces), i.e.,

$$H_d(\mathbf{q}) = \sum_i h_{ii} + \sum_i \sum_{j>i} h_{ij}. \tag{2.2}$$

Here, the elements are defined as

$$h_{ii} = |i\rangle[K(\dot{\mathbf{q}}) + V_{ii}(\mathbf{q})]\langle i|, \tag{2.3}$$

where K is the kinetic energy term for the nuclear coordinates $\mathbf{q}$, and

$$h_{ij} = V_{ij}(\mathbf{q})(|i\rangle\langle j| + |j\rangle\langle i|), \tag{2.4}$$

where the off-diagonal coupling elements satisfy the Hermitian relation $V_{ij} = V_{ji}^*$. Unlike the usual adiabatic barrier crossing problem, the potential energy terms V_{ii} in the elements h_{ii} describe ''simple'' diabatic surfaces having, or not having, potential wells. Therefore, in the most general sense the quantum reactive dynamics is induced by a transition between different diabatic surfaces instead of taking place on a single adiabatic surface (e.g., a double well formed on the lowest adiabatic potential surface). This formulation of the problem is completely general.

Following a prescription originally proposed by Langer at zero temperature[18] and later employed in various adiabatic quantum rate calculations,[20,21] the desired electron transfer rate constant k_{ET} can be approximated in terms of equilibrium quantities by

$$k_{\mathrm{ET}} \simeq -\frac{1}{\hbar\beta}\,\mathrm{Im}\,\frac{\ln Z}{Z_0} = \frac{1}{\hbar\beta}\frac{Z_b}{Z_0}, \tag{2.5}$$

with Z_0 being the partition function of the reactant state, Z is the overall system partition function, and Z_b is loosely defined here as the ''barrier'' contribution to the partition function. The final states are assumed to have sufficient density that k_{ET} can be interpreted as the rate of exponential tunneling decay.

Provided the effective barrier height is significantly larger than the thermal energy in the diabatic wells, the steepest descent method can be applied to evaluate the imaginary part of the partition function Z which leads to the instanton solution in Eq. (2.5). A number of aspects of the instanton solution in various limits have been elaborated by others (see, e.g., Refs. 32–37). The focus of the present work, however, is on a *computational* methodology to evaluate the instanton rate constant in the most general case which *bridges* the adiabatic and nonadiabatic (golden rule) limits of ET. An assumption has been made in formulating this approach that Eq. (2.5) is a valid approximation in *all* limits of the ET problem. While numerical and analytical results presented below will support this assumption, it has not been derived from first principles.

The stationary path of the Hamiltonian in Eq. (2.1) consists of the nuclear instanton trajectory and the self-consistent electronic wave function propagation in imaginary time arising from the coupling of the two subsystems. This self-consistency arises from the fact that the equation of motion for the nuclear coordinates depends on the imaginary time evolution of the multilevel wave function which, in turn, depends on the instanton trajectory. A similar challenge, albeit for real time dynamics, has been encountered previously in the study of the dynamics of coupled classical-quantum systems.[24,26,27] Pechukas was the first to provide a rigorous prescription for the self-consistent stationary phase classical-like trajectory and time-dependent wave function based on Feynman's path integral formulation of quantum dynamics.[28,29] This elegant theory has since been developed into various approximation algorithms for nonadiabatic dynamics.[24–27] A Pechukas-type theory will now be developed for the nonadiabatic quantum instanton solution [cf. Eqs. (2.1) and (2.5)] so as to provide a means for calculating the electron transfer rate constant under general conditions.

The trace operation of the quantum Boltzmann operator for the Hamiltonian in Eq. (2.1) involves a summation over all the electronic diabatic surfaces and an integration over all nuclear coordinates. Importantly, however, this operation must be rewritten to expose the terms involving diabatic state transitions which contribute to the imaginary part of the partition function. By inserting complete sets of diabatic and coordinate basis states, the tunneling rate from one diabatic surface, denoted by $|\mu\rangle$, to another diabatic surface, denoted by $|\nu\rangle$, is related to the following quantity:

$$\begin{aligned} Z_{\mu,\nu} = \int d\mathbf{r} \int d\mathbf{r}' \int d\mathbf{q} \int d\mathbf{q}' \langle \mu, \mathbf{q}, \mathbf{r}| \\ \times \exp(-\beta H/2)|\nu, \mathbf{q}', \mathbf{r}'\rangle\langle \nu, \mathbf{q}', \mathbf{r}'| \\ \times \exp(-\beta H/2)|\mu, \mathbf{q}, \mathbf{r}\rangle, \end{aligned} \tag{2.6}$$

where $\mathbf{q}$ and $\mathbf{q}'$ are located near the wells of diabatic surfaces $|\mu\rangle$ and $|\nu\rangle$, respectively. It should be noted that the two imaginary time propagators in Eq. (2.6) are the same. [See also Eq. (C2) of Ref. 37, p. 145.]

Next, the propagator is separated into the wave function propagation of the diabatic levels and the propagation arising from H_0, which is the Hamiltonian excluding H_d, giving

$$\begin{aligned} Z_{\mu,\nu} = \int \mathscr{D}\mathbf{r}(\tau) \int \mathscr{D}\mathbf{q}(\tau) \exp\{-S_0[\mathbf{q}(\tau), \mathbf{r}(\tau)]/\hbar\} \\ \times T_{\mu\nu}[\hbar\beta, \hbar\beta/2, \mathbf{q}(\tau)] T_{\nu\mu}[\hbar\beta/2, 0, \mathbf{q}(\tau)]. \end{aligned} \tag{2.7}$$

Here, $S_0[\mathbf{q}(\tau), \mathbf{r}(\tau)]$ is the action functional excluding the contribution from H_d, i.e.,

$$\begin{aligned} S_0 = \int_0^{\hbar\beta} d\tau \{\tfrac{1}{2}\dot{\mathbf{q}}(\tau) \cdot \mathbf{m} \cdot \dot{\mathbf{q}}(\tau) + V_{\mathrm{int}}[\mathbf{q}(\tau), \mathbf{r}(\tau)]\} \\ + S_b[\mathbf{r}(\tau)], \end{aligned} \tag{2.8}$$

where $\mathbf{m}$ is the mass matrix and S_b is the action functional of the bath.

The quantity $T_{\nu\mu}$ is the overlap between the initial diabatic state $|\mu\rangle$ and the final diabatic state $|\nu\rangle$. In an explicit form, the Bloch equation can be introduced to describe the evolution of diabatic wave function, i.e.,

$$-\frac{\partial u(\tau, \tau')}{\partial \tau} = H_d[\mathbf{q}(\tau)] u(\tau, \tau') \tag{2.9}$$

so that

$$T_{\nu\mu}[\tau, \tau', \mathbf{q}(\tau)] = \langle \nu | u(\tau, \tau') | \mu \rangle, \tag{2.10}$$

which is a functional of the system nuclear path $\mathbf{q}(\tau)$ and the imaginary time interval satisfies $0 \leqslant \tau \leqslant \hbar\beta$.

To facilitate further analysis, the bath average of a functional $f[\mathbf{q}(\tau),\mathbf{r}(\tau)]$ is introduced here as

$$\langle f(\tau)\rangle_b = \frac{\int \mathscr{D}\mathbf{r}(\tau') f[\mathbf{q}(\tau),\mathbf{r}(\tau)] \exp\{-S_b[\mathbf{r}(\tau')]/\hbar - \int_0^{\hbar\beta} d\tau' V_{\rm int}[\mathbf{q}(\tau'),\mathbf{r}(\tau')]/\hbar\}}{\int \mathscr{D}\mathbf{r}(\tau') \exp\{-S_b[\mathbf{r}(\tau')]/\hbar - \int_0^{\hbar\beta} d\tau' V_{\rm int}[\mathbf{q}(\tau'),\mathbf{r}(\tau')]/\hbar\}}, \tag{2.11}$$

and the quantum average over the diabatic basis for $\tau \leqslant \hbar\beta/2$ is denoted by

$$\langle f(\tau)\rangle_d = \frac{\langle \nu|u(\hbar\beta/2,\tau) f(\tau) u(\tau,0)|\mu\rangle}{\langle \nu|u(\hbar\beta/2,\tau) u(\tau,0)|\mu\rangle}, \tag{2.12}$$

or, if $\tau \geqslant \hbar\beta/2$, then

$$\langle f(\tau)\rangle_d = \frac{\langle \nu|u(\hbar\beta,\tau) f(\tau) u(\tau,\hbar\beta/2)|\mu\rangle}{\langle \nu|u(\hbar\beta,\tau) u(\tau,\hbar\beta/2)|\mu\rangle}. \tag{2.13}$$

In Eqs. (2.12) and (2.13), the denominators are independent of the variable τ and $f(\tau)$ is in general a matrix. Both the quantum average and the solvent average are carried out by assuming a particular nuclear path $\mathbf{q}(\tau)$ and are thus functionals of the nuclear paths.

With the definition of Eq. (2.11) in hand, one can rewrite the path integral in Eq. (2.7) as

$$Z_{\mu,\nu} = \int \mathscr{D}\mathbf{q}(\tau) \exp\{-S_{\rm eff}[\mathbf{q}(\tau)]/\hbar\}, \tag{2.14}$$

with the effective action functional given by

$$\begin{aligned} S_{\rm eff}[\mathbf{q}(\tau)] = & \int_0^{\hbar\beta} d\tau \{\tfrac{1}{2}\dot{\mathbf{q}}(\tau)\cdot\mathbf{m}\cdot\dot{\mathbf{q}}(\tau)\} + W_b[\mathbf{q}(\tau)] \\ & - \hbar(\ln\{T_{\mu\nu}[\hbar\beta,\hbar\beta/2,\mathbf{q}(\tau)]\} \\ & + \ln\{T_{\nu\mu}[\hbar\beta/2,0,\mathbf{q}(\tau)]\}), \end{aligned} \tag{2.15}$$

where

$$\begin{aligned} W_b[\mathbf{q}(\tau)] = -\hbar \ln\Bigg(\int \mathscr{D}\mathbf{r}(\tau) \exp\Bigg\{ & -S_b[\mathbf{r}(\tau)]/\hbar \\ & - \int_0^{\hbar\beta} d\tau V_{\rm int}[\mathbf{q}(\tau),\mathbf{r}(\tau)]/\hbar \Bigg\}\Bigg). \end{aligned} \tag{2.16}$$

Application of the steepest descent approximation to Eq. (2.14) leads to the equation of motion for the nuclear coordinates

$$\mathbf{m}\cdot\frac{d^2\mathbf{q}(\tau)}{d\tau^2} = \left\langle \frac{\partial H_d[\mathbf{q}(\tau)]}{\partial \mathbf{q}(\tau)} \right\rangle_d + \left\langle \frac{\partial V_{\rm int}[\mathbf{q}(\tau)]}{\partial \mathbf{q}(\tau)} \right\rangle_b \tag{2.17}$$

which is to be solved together with Eqs. (2.9) and (2.11)–(2.13) to obtain the nonadiabatic instanton solution. Because of the time reversal property of the amplitudes $T_{\nu\mu}$ and $T_{\mu\nu}$, the instanton trajectory is symmetric with respect to the imaginary time $\hbar\beta/2$, and so is the wave function. The self-consistent condition for the many-body nonadiabatic instanton solution is twofold; the coupling between the diabatic states propagation and the instanton trajectory, and the coupling between the bath distribution and the instanton trajectory.

In order to complete the instanton analysis, the second order functional derivative must be evaluated along the instanton trajectory. This procedure is numerically best implemented for a discretized path, i.e.,

$$\begin{aligned} \frac{\delta^2 S}{\delta\mathbf{q}_i \delta\mathbf{q}_j} = & \frac{\mathbf{m}}{\epsilon^2}(2\delta_{i,j} - \delta_{i,j+1} - \delta_{i,j-1}) \\ & + \delta_{i,j}\left\langle \frac{\partial^2 H_d[\mathbf{q}(\tau)]}{\partial\mathbf{q}_i \partial\mathbf{q}_i} \right\rangle_d + \epsilon \mathbf{C}_{d,ij} \\ & + \delta_{i,j}\left\langle \frac{\partial^2 V_{\rm int}[\mathbf{q}(\tau)]}{\partial\mathbf{q}_i \partial\mathbf{q}_i} \right\rangle_b + \epsilon \mathbf{C}_{b,ij}, \end{aligned} \tag{2.18}$$

where the indices i and j denote two different discretized imaginary time slices, $\mathbf{q}_i$ and $\mathbf{q}_j$ are the corresponding nuclear coordinates along the instanton path, and $\epsilon = \hbar\beta/P$, with P being the number of discretizations. Here, $\mathbf{C}_{b,ij}$, the bath fluctuation correlation matrix, is given by

$$\begin{aligned} \mathbf{C}_{b,ij} = & \left\langle \frac{\partial V_{\rm int}[\mathbf{q}(\tau)]}{\partial\mathbf{q}_i} \frac{\partial V_{\rm int}[\mathbf{q}(\tau)]}{\partial\mathbf{q}_j} \right\rangle_b \\ & - \left\langle \frac{\partial V_{\rm int}[\mathbf{q}(\tau)]}{\partial\mathbf{q}_i} \right\rangle_b \left\langle \frac{\partial V_{\rm int}[\mathbf{q}(\tau)]}{\partial\mathbf{q}_j} \right\rangle_b, \end{aligned} \tag{2.19}$$

and, $\mathbf{C}_{d,ij}$, the quantum fluctuation correlation matrix, is given by

$$\begin{aligned} \mathbf{C}_{d,ij} = & \left\langle \frac{\partial H_d[\mathbf{q}(\tau)]}{\partial\mathbf{q}_i} u(\tau_i,\tau_j) \frac{\partial H_d[\mathbf{q}(\tau)]}{\partial\mathbf{q}_j} \right\rangle_d \\ & - \left\langle \frac{\partial H_d[\mathbf{q}(\tau)]}{\partial\mathbf{q}_i} \right\rangle_d \left\langle \frac{\partial H_d[\mathbf{q}(\tau)]}{\partial\mathbf{q}_j} \right\rangle_d. \end{aligned} \tag{2.20}$$

The dimensionality implicit in the above equations is such that $\delta^2 S/\delta\mathbf{q}_i\delta\mathbf{q}_j$ is a matrix of dimension $N\times P$. When diagonalizing this matrix, there will be a negative eigenvalue giving arise to the imaginary part of the partition function, and a zero eigenvalue corresponding to the translationally invariant mode.[20] The existence of a zero eigenvalue is an indication of a true instanton solution. The removal of the zero eigenvalue requires the proper normalization, which is explained in Appendix A.

After the preceding analysis is carried out, one arrives at the nonadiabatic instanton approximation for the electron transfer rate constant, i.e.,

$$k_{\mathrm{ET}} \simeq \left(\frac{W}{2\pi\hbar D}\right)^{1/2} \exp(-S_{\mathrm{inst}}/\hbar), \tag{2.21}$$

where W and S_{inst} are the work and the action, respectively, along the instanton trajectory, and D is a properly normalized determinant of the matrix in Eq. (2.18), excluding the zero eigenvalue (cf. Appendix A).

In light of the preceding discussion, there are several observations which can be made.

(a) Assuming a single diabatic surface in the Hamiltonian [Eq. (2.1)] which contains a single barrier, one recovers the well-known single surface instanton solution. In the case of a multilevel system, if the coupling is strong enough so that the nuclear system always moves on the lowest-lying adiabatic potential energy surface, the present nonadiabatic instanton solution can be shown to reduce to the single surface, adiabatic limit.

(b) In the limit of two weakly coupled diabatic surfaces, the Bloch equation in Eq. (2.9) can be linearized, resulting in a transition amplitude $T_{\nu\mu}[\tau,\tau',\mathbf{q}(\tau)]$ which is proportional to the off-diagonal coupling element of the H_d matrix. This limit of the theory thus recovers the golden rule ET rate constant.[3,38]

(c) If the solvent is treated as being classical, the bath paths $\mathbf{r}(\tau)$ shrink to a point and Eq. (2.11) can be rewritten as the configurational integral

$$\langle f(\tau)\rangle_b = \frac{\int d\mathbf{r} f[\mathbf{q}(\tau),\mathbf{r}]\exp\{-\beta V_b(\mathbf{r}) - \int_0^{\hbar\beta} d\tau' V_{\mathrm{int}}[\mathbf{q}(\tau'),\mathbf{r}]/\hbar\}}{\int d\mathbf{r}\, \exp\{-\beta V_b(\mathbf{r}) - \int_0^{\hbar\beta} d\tau' V_{\mathrm{int}}[\mathbf{q}(\tau'),\mathbf{r}]/\hbar\}}, \tag{2.22}$$

where $V_b(\mathbf{r})$ is the potential function for the bath variables.

(d) The Gaussian bath has a wide appeal in studying solvent effects in condensed media.[23,39] Given a harmonic bath and a bilinear coupling between system and bath, one can explicitly integrate out the bath modes in Eqs. (2.11) and (2.16), giving the equation of motion for the instanton trajectory in Eq. (2.17) as

$$\mathbf{m}\cdot \frac{d^2\mathbf{q}(\tau)}{d\tau^2} = \left\langle \frac{\partial H_d(\tau)}{\partial \mathbf{q}(\tau)} \right\rangle_d - \frac{1}{\hbar}\int_0^{\hbar\beta} d\tau' \mathbf{c}(|\tau-\tau'|)\cdot \mathbf{q}(\tau'), \tag{2.23}$$

where $\mathbf{c}(|\tau-\tau'|)$ is the imaginary time correlation function matrix

$$\mathbf{c}(|\tau-\tau'|) = \frac{\hbar}{\pi}\int_0^{\infty} d\omega \mathbf{J}(\omega)\, \frac{\cosh(\hbar\beta\omega/2-\omega|\tau-\tau'|)}{\sinh(\hbar\beta\omega/2)}, \tag{2.24}$$

and $\mathbf{J}(\omega)$ is the bath spectral density matrix, related to the elements of the classical friction tensor $\eta_{ij}(t)$ by

$$\eta_{ij}(t) = \frac{2}{\pi}\int_0^{\infty} d\omega\, \frac{\mathbf{J}_{ij}(\omega)}{\omega} \cos\,\omega t. \tag{2.25}$$

(e) In the case of a two-state system with a constant coupling between the states, quadratic diabatic surfaces, and a Gaussian bath, the Hamiltonian becomes the spin-boson model which has been often implemented in the study of electron transfer (see, e.g., Ref. 39).

III. RESULTS

In this section, practical algorithms are described to solve the equations in the nonadiabatic instanton theory, and numerical calculations are carried out for the spin-boson model in order to apply the theory to a well-known example. In spite of its apparent simplicity, the spin-boson Hamiltonian serves as the primary model for investigating nonadiabatic transitions because of its physical richness. Moreover, the assumption of a Gaussian bath in the spin-boson model removes the self-consistent requirement of the instanton path and the solvent distribution, thus greatly simplifying the numerical calculations. (It should be noted, however, that there is still the self-consistent requirement of the instanton path with the nonadiabatic state propagation.) There is no fundamental problem associated with the former self-consistency issue and a subsequent publication will deal with it explicitly for multidimensional, nonlinear potentials.

The major numerical effort in the present theory is to find the instanton trajectory, that is, to solve Eq. (2.17) simultaneously along with the Bloch equation in Eq. (2.9). Given the force, the equation of motion in Eq. (2.17) is solved iteratively for a discretized instanton path. It must be pointed out, however, that the instanton trajectory is neither a minimum nor a maximum of the action, but an extremum of the action. Consequently, an iterative method has the possibility of converging the instanton in real space to the minimum of a double-well potential, which is a trivial solution to the stationary condition in Eq. (2.17). To prevent this behavior in the iteration method, it is helpful to choose a good initial input trajectory to approximate the true instanton solution. An educated guess is the instanton solution for the adiabatic surface, which works particularly well in the strong coupling region. In the intermediate coupling region, a trajectory solved for a larger coupling constant can be employed as an input to the algorithm. In the weak coupling region, the adiabatic instanton solution for the cusped barrier is a good initial guess (cf. Appendix B). The rate of convergence depends on the discretization number and the initial input. Generally, it has been found that around 10^3 iterations will yield convergence.

Given a nuclear path $\mathbf{q}(\tau)$, the Bloch equation Eq. (2.9) is solved by numerical integration. At each time step $\epsilon=\hbar\beta/P$, the Hamiltonian H_d at that time is diagonalized and propagated for one step. The initial state $|\mu\rangle$ and the final state $|\nu\rangle$ are the right and the left diabatic surfaces, respec-

tively. With the electronic wave function in hand, one returns to the calculation of the instanton trajectory, which in turn leads to a new electronic wave function. This procedure forms a loop until self-consistency is reached. In the examples studied so far, the convergence of the wave function and the nonadiabatic instanton trajectory was always achieved in less than 100 iterations.

Once the instanton solution is found, the fluctuation matrix of Eq. (2.18) is computed and diagonalized. A vanishingly small eigenvalue will assure a satisfactory stationarity condition [Eq. (2.17)] and a negative eigenvalue indicates the metastability of the particular solution (i.e., the "barrier" partition function). The prefactor D in Eq. (2.21) can thus be calculated, and the action S and work W computed, hence yielding the instanton rate constant. In summary, the complete nonadiabatic instanton algorithm consists of following steps:

(1) An approximate instanton trajectory is used as an input.
(2) The stationary condition in Eq. (2.17) is iterated to a converged trajectory for a given electronic wave function.
(3) The Bloch equation in Eq. (2.9) is solved numerically for a given nuclear path.
(4) Steps (2) and (3) are repeated until convergence is reached.
(5) The instanton rate constant is computed from Eq. (2.21).

As stated before, in order to test the method the spin-boson model was studied. In one particular form, this model is described by the Hamiltonian

$$H=\tfrac{1}{2}m\dot{q}^2+\Delta\sigma_x+\tfrac{1}{2}m\omega^2(q-\sigma_z q_0)^2 + \sum_{j=1}^{N} c_j q x_j+\frac{1}{2}\sum_{j=1}^{N}(\dot{x}_j^2+\omega_j^2 x_j^2)+\sum_{j=1}^{N}\frac{c_j^2}{2\omega_j^2}q^2, \tag{3.1}$$

where σ is the Pauli spin matrix, Δ is one-half the tunnel splitting, and the modes $\{x\}$ constitute the Gaussian bath. The parameters were chosen in the present case to be $\hbar=1.0$, $\omega=1.0$, $m=1.0$, $\beta=5.0$, $q_0=5.0$. A discretization parameter of $P=200$ to $P=400$ was used in the calculations, depending on the temperature. The parameters of the bath were chosen so that its spectral density, given in discrete form by[23]

$$J(\omega)=\frac{\pi}{2}\sum_{j=1}^{N}\frac{c_j^2}{\omega_j}\delta(\omega-\omega_j), \tag{3.2}$$

reproduced an appropriate friction kernel in the classical limit.

As a first calculation, a frictionless spin-boson model was used to verify that the method works in well-known limits and to examine the numerical characteristics of the algorithm. In Fig. 1, the electron transfer rate constant is plotted as a function of the coupling constant Δ on a logarithmic scale. In the strong coupling region (i.e., large Δ) the nonadiabatic instanton rate approaches the adiabatic rate (dot–dashed line) because the coupling is strong enough that the quantum transition takes place on the lower adiabatic surface. In the weak coupling region, the nonadiabatic rate

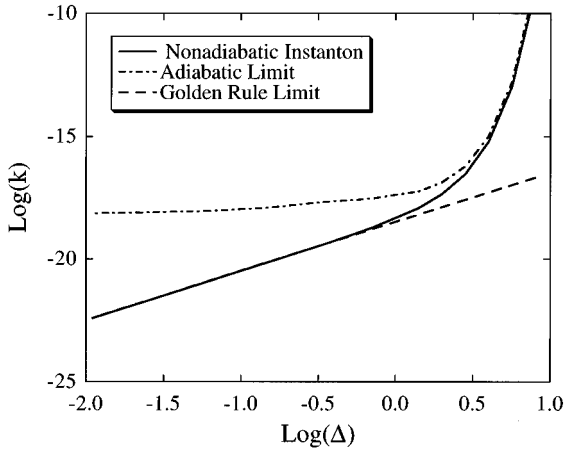

FIG. 1. A logarithmic plot of the rate constant vs the nonadiabatic coupling constant Δ for the Hamiltonian given in Eq. (3.1). For comparison, the golden rule prediction from Eq. (3.3) is plotted as a dashed line, and the adiabatic rate constant is plotted as a dot–dashed line.

obviously becomes proportional to the Δ^2, as predicted by the golden rule (dashed line). The golden rule rate in this simple case is given analytically by

$$k_{\mathrm{ET}}=\frac{\Delta^2}{\hbar}\sqrt{\frac{\pi\sinh(b/2)}{2E_a\hbar\omega}}\exp\left[-\beta E_a\frac{\tanh(b/4)}{(b/4)}\right], \tag{3.3}$$

where the activation energy is $E_a=m\omega^2 q_0^2/2$ and $b=\hbar\beta\omega$. The adiabatic tunneling rate reaches a plateau, which is the instanton rate for a cusped double-well discussed in Appendix B. It should be noted that even in this simple limit of the spin-boson model, the method is capable of dealing with an arbitrary nonadiabatic coupling strength, bridging the adiabatic and nonadiabatic limits of the ET dynamics. It should also be noted that numerically exact methods exist for studying the quantum dynamics of spin-boson model for all values of the relevant parameters.[4–9]

In the adiabatic limit, the instanton solution exists only in the quantum tunneling dominated region, but not in the activated barrier crossing region (for a discussion of these limits, see the review in Ref. 40). The crossover to the instanton rate is given by the well-known criterion $\hbar\beta\omega_b>2\pi$, with ω_b being the adiabatic barrier frequency. A path integral quantum transition state theory[10–13] calculation can be performed above the crossover region in the adiabatic limit which will bridge with the instanton solution. Furthermore, in a complex system all that is required is that a *single* nuclear mode be tunneling in order for the instanton solution to exist. In the nonadiabatic limit, the weak coupling induces a nonadiabatic transition in a small region near the crossing of the diabatic surfaces, thus leading to a sharp barrier curvature in the adiabatic surface which insures the validity of the instanton approach. Therefore, in the golden rule region the steepest descent approximation is always valid, even in the classical limit of the nuclear coordinates.

To further illustrate the characteristics of the nonadiabatic instanton solution, the following results are presented to explore different aspects of the transition from the nona-

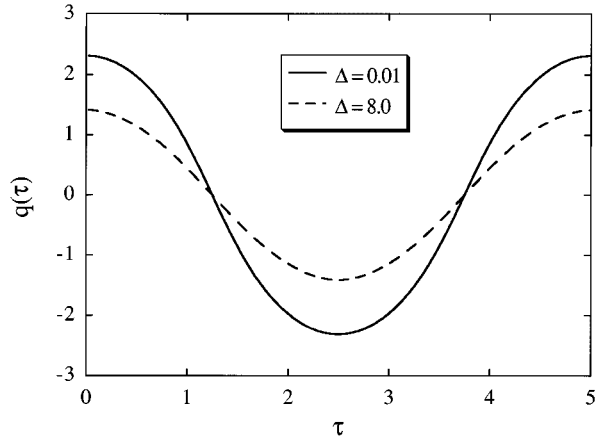

FIG. 2. The nonadiabatic instanton trajectories plotted for $\Delta=0.1$ and $\Delta=8.0$ as a function of the imaginary time.

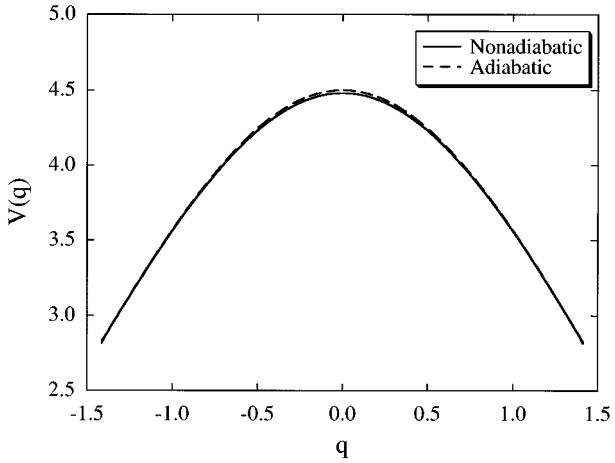

FIG. 4. The effective nonadiabatic potential defined in Eq. (3.4) plotted along with the adiabatic potential surface for $\Delta=8.0$.

diabatic limit to the adiabatic limit:

(a) The nonadiabatic instanton trajectories are shown for $\Delta=0.01$ and $\Delta=8.0$ in Fig. 2. Obviously, the instanton trajectory shrinks as the coupling constant increases. On the other hand, the nonadiabatic trajectory becomes independent of the coupling constant as the latter becomes smaller.

(b) Assuming the electronic wave function has been determined, one can define an effective potential surface for the instanton trajectory as

$$V_{\text{eff}}[q(\tau)]=\langle V[q(\tau)]\rangle_d, \tag{3.4}$$

the derivative of which gives the nonadiabatic instanton force. For comparison, one can also evaluate the adiabatic potential by diagonalizing the Pauli spin matrix in Eq. (3.1) for fixed values of the coordinate q. The effective potential is plotted along with the adiabatic potential surface for $\Delta=0.01$ in Fig. 3 and for $\Delta=8.0$ in Fig. 4. As one can observe from Fig. 4, the adiabatic potential surface is a very good approximation to the effective potential surface for large coupling constant, whereas the cusped adiabatic potential surface at the small coupling constant in Fig. 3 is very different from the rounded effective potential.

(c) The evolution of spin population is plotted for $\Delta=0.01$ in Fig. 5 and for $\Delta=8.0$ in Fig. 6. As has been stated earlier, in the adiabatic region the relative population on the two diabatic surfaces is such that its state vector forms the adiabatic surface. In the golden rule region, the transition is confined in a small region near the crossing point of the diabatic surfaces and happens rather dramatically.

Next, the dissipative quantum tunneling region was investigated by adding a Gaussian bath to the spin-boson model [cf. Eq. (3.1)]. The bath spectral density was chosen in the Drude approximation, i.e.,

$$J(\omega)=\eta\omega\,\frac{\omega_c^2}{\omega^2+\omega_c^2}, \tag{3.5}$$

where the friction strength η was 1.0 and the inverse of the memory time scale, ω_c, was 1.0. In Fig. 7, the quantum rate

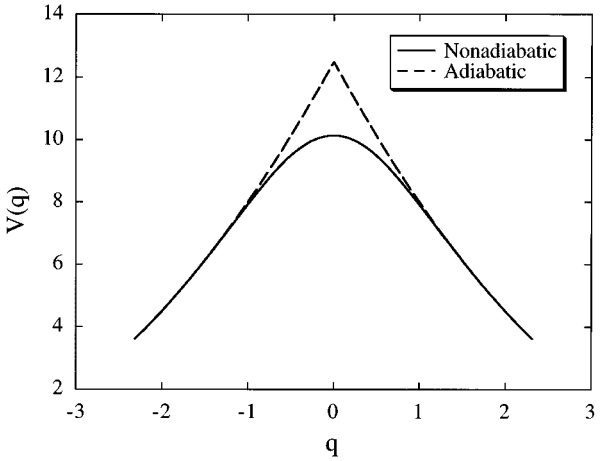

FIG. 3. The effective nonadiabatic potential defined in Eq. (3.4) plotted along with the adiabatic potential surface for $\Delta=0.01$.

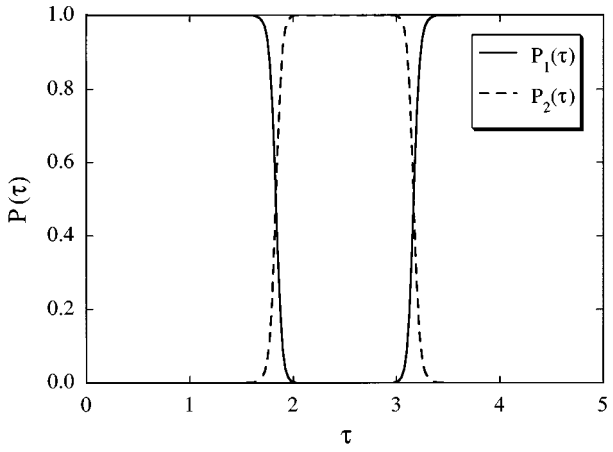

FIG. 5. The evolution of the population on the two diabatic surfaces plotted for $\Delta=0.01$.

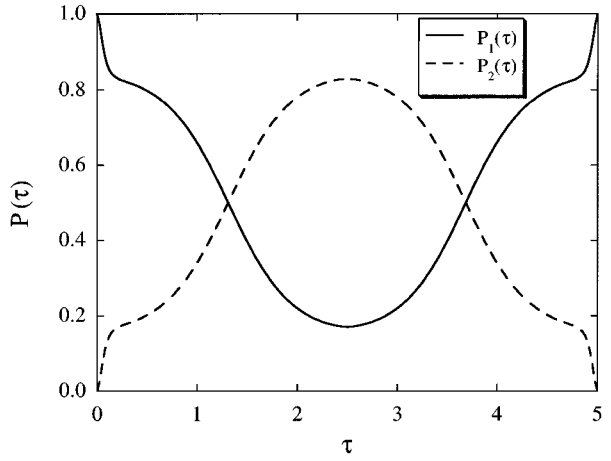

FIG. 6. The evolution of the population on the two diabatic surfaces plotted for $\Delta=8.0$.

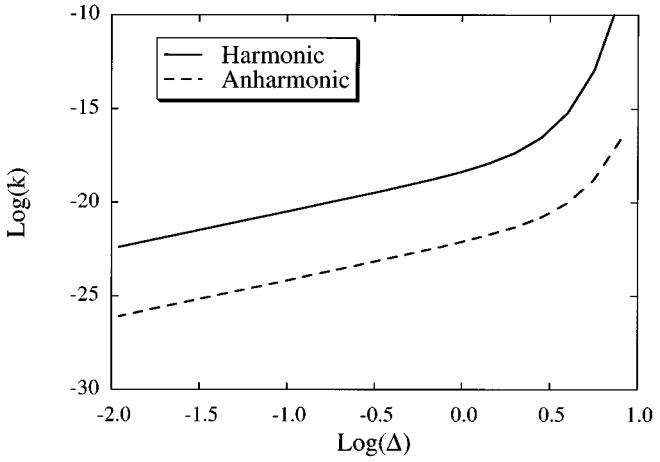

FIG. 8. The rate constant in an anharmonic diabatic potential given in Eq. (3.6) plotted as a function of the nonadiabatic coupling constant.

in the dissipative bath is plotted as a function of the coupling constant and compared with the nondissipative rate. As is expected, the tunneling rate is reduced by a substantial amount because of the bath dissipation. In addition, the dissipative suppression is stronger in the nonadiabatic limit than in the adiabatic limit.

Finally, the effects of anharmonicity on the quantum rate constant were studied by assuming diabatic surfaces defined by

$$V_{ii}(q)=\tfrac{1}{2}m\omega^2(q-\sigma_z q_0)^2+g(q-\sigma_z q_0)^4, \tag{3.6}$$

where $g=0.01$ and the other parameters are taken to be the same as in Eq. (3.1). In Fig. 8, the rate constant for the frictionless system is plotted as a function of the nonadiabatic coupling constant Δ. Clearly, introducing the anharmonicity reduces the tunneling rate and the reduction is more drastic in the adiabatic region than in the nonadiabatic region. This example illustrates the real strength of the nonadiabatic instanton method, i.e., it is not limited to quadratic diabatic surfaces.

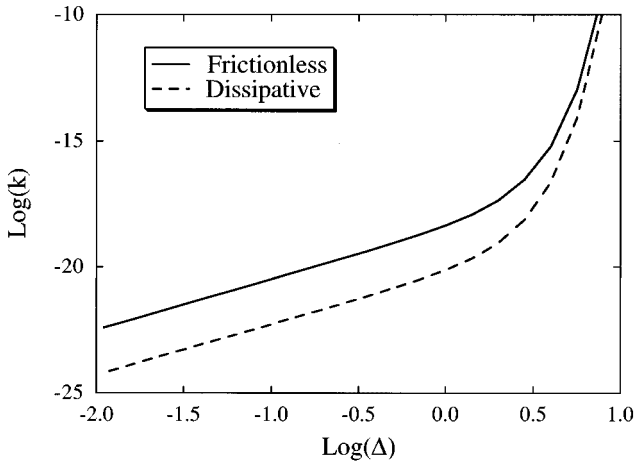

FIG. 7. The dissipative rate constant with the bath spectral density given in Eq. (3.5) plotted as a function of the nonadiabatic coupling constant.

IV. CONCLUSIONS

In this paper, a computational methodology for determining electron transfer rates has been developed. The approach is based on the instanton expression for quantum rate constants combined with a nonadiabatic dynamics formalism for treating the imaginary time instanton dynamics with nonadiabatic transitions. The formulation is completely general and thereby capable of treating nonlinear diabatic potential energy surfaces and multiple electronic states. It also provides a computational method for bridging the adiabatic and nonadiabatic limits of electron transfer processes. The theory was tested for the well-known spin-boson model, obtaining excellent agreement with analytical predictions in both the adiabatic and nonadiabatic (golden rule) limits. In addition, it was shown that both dissipation and nonlinearity in the diabatic potentials can readily be included in the calculations and may have large effects on the rate constant. In future publications, the nonadiabatic instanton method will be further developed and applied to study electron transfer processes in realistic systems.

ACKNOWLEDGMENTS

This research was supported by the National Science Foundation (CHE-9158079) and (CHE-9410608) and by the Office of Naval Research. G.A.V. is a recipient of a National Science Foundation Presidential Young Investigator Award, a David and Lucile Packard Fellowship in Science and Engineering, an Alfred P. Sloan Foundation Research Fellowship, and a Camille Dreyfus Teacher–Scholar Award.

APPENDIX A: EVALUATION OF THE INSTANTON PREFACTOR

In this section, the prefactor D in Eq. (2.21) is explicitly expressed as a normalized determinant of the matrix in Eq. (2.18). For a free particle, the matrix describing the quantum path fluctuations is given by

$$\frac{\delta^2 S}{\delta \mathbf{q}_i \delta \mathbf{q}_j} = \frac{m}{\epsilon^2}\,(2\delta_{i,j} - \delta_{i,j+1} - \delta_{i,j-1}), \tag{A1}$$

where $\epsilon = \hbar\beta/P$. A normal-mode transformation immediately leads to the eigensolutions of the matrix in Eq. (A1), i.e.,

$$\lambda_l = 2[1 - \cos(2\pi l/P)], \tag{A2}$$

where the index l ranges from $-(P-1)/2$ to $(P-1)/2$. Obviously, $l=0$ gives a zero eigenvalue which corresponds to the translational invariance of the free particle space. Removal of this zero eigenvalue leads to the condition

$$\prod_{l\neq 0} \lambda_l = P^2 \tag{A3}$$

which recovers the correct free particle density. Thereby, the instanton matrix in Eq. (2.18) is normalized to the free particle prefactor, giving

$$D = \lim_{P\to\infty} \frac{1}{P^2}\,\det{}'\left(\frac{\epsilon^2}{m}\,\frac{\delta^2 S}{\delta \mathbf{q}_i \delta \mathbf{q}_j}\right), \tag{A4}$$

where $\det'$ stands for the value of the determinant with the zero eigenvalue removed. The above equation defines the prefactor in Eq. (2.21).

APPENDIX B: THE INSTANTON SOLUTION FOR THE CUSPED POTENTIAL

In the weak coupling limit of the spin-boson model for electron transfer, the ground state adiabatic potential surface approaches a cusped parabolic double well. For such a system, the instanton rate can be exactly calculated.[33] For simplicity, a one-dimensional symmetric double well potential is considered here, given by

$$V(q) = \tfrac{1}{2}\, m\omega^2 [q - \mathrm{sign}(q) q_0]^2, \tag{B1}$$

where the symbol $\mathrm{sign}(q)$ stands for the sign of q. The action functional for a quantum particle embedded in a Gaussian bath then reads

$$S[q(\tau)] = \int_0^{\hbar\beta} d\tau \{\tfrac{1}{2}\, m\dot{q}(\tau)^2 + V[q(\tau)]\} - \frac{1}{2\hbar}\int_0^{\hbar\beta}\int_0^{\hbar\beta} d\tau' c(|\tau-\tau'|) q(\tau') q(\tau), \tag{B2}$$

where $c(|\tau-\tau'|)$ is the correlation function given by Eq. (2.24).

The quantum rate problem for this potential is most easily solved by properly connecting the two analytical solutions of the wells at the cusp. The resulting instanton rate constant is given by

$$k = 4\omega^2 q_0 \sqrt{\frac{m}{2\pi\hbar^2\beta}}\,\frac{\Sigma_{\mathrm{odd}} a_n}{\sqrt{\Sigma(-1)^n a_n}}\,\exp\left(-\beta\,\frac{m q_0^2}{2\Sigma_{\mathrm{even}} a_n}\right), \tag{B3}$$

where the factor a_n is defined by

$$a_n = \frac{1}{\Omega_n^2 + \omega^2 - \beta\tilde{c}_n/m}. \tag{B4}$$

Here, $\Omega_n = 2\pi n/\hbar\beta$ and $\tilde{c}_n$ is given by

$$\tilde{c}_n = \frac{1}{\hbar\beta}\int_0^{\hbar\beta} d\tau e^{i\Omega_n\tau} c(|\tau|). \tag{B5}$$

In the case of a frictionless cusped double-well, the rate constant k can be expressed in a closed form as

$$k = 2\omega q_0 \sqrt{\frac{m\omega}{\hbar}}\,\frac{\sinh^2(b/4)}{\sinh^{1/2}(b/2)}\,\exp\left[-\beta E_a\,\frac{\tanh(b/4)}{(b/4)}\right]. \tag{B6}$$

The exponential factor in the above equation is the same as the one in the golden rule expression [Eq. (3.3)], whereas the prefactor is by no means the same. Thereby, it is necessary to introduce the nonadiabatic coupling mechanism in order to obtain the correct limit for the electron transfer dynamics. The above equations, however, can serve as a good initial guess for the nonadiabatic instanton algorithm (cf. Sec. III).

[1] R. A. Marcus and N. Sutin, Biochim. Biophys. Acta. **811**, 265 (1985).
[2] The literature on the subject of electron transfer is vast. Reference 1 is a representative review article.
[3] J. S. Bader, R. A. Kuharski, and D. Chandler, J. Chem. Phys. **93**, 230 (1990).
[4] C. H. Mak and D. Chandler, Phys. Rev. A **41**, 5709 (1990).
[5] C. H. Mak and D. Chandler, Phys. Rev. A **44**, 2352 (1991).
[6] R. Egger and C. H. Mak, J. Chem. Phys. **99**, 2541 (1993).
[7] R. Egger, C. H. Mak, and U. Weiss, J. Chem. Phys. **100**, 2651 (1994).
[8] D. Makarov and N. Makri, Phys. Rev. A **48**, 3626 (1993).
[9] D. Makarov and N. Makri, Chem. Phys. Lett. **221**, 482 (1994).
[10] G. A. Voth, D. Chandler, and W. H. Miller, J. Chem. Phys. **91**, 7749 (1989).
[11] G. A. Voth, Chem. Phys. Lett. **270**, 289 (1990).
[12] G. A. Voth, J. Phys. Chem. **97**, 8365 (1993), for a review of path integral quantum transition state theory, see this paper.
[13] M. J. Gillan, J. Phys. C **20**, 3621 (1987).
[14] J. N. Gehlen, D. Chandler, H. J. Kim, and J. T. Hynes, J. Phys. Chem. **96**, 1748 (1992).
[15] J. N. Gehlen and D. Chandler, J. Chem. Phys. **97**, 4958 (1992).
[16] X. Song and A. A. Stuchebrukhov, J. Chem. Phys. **99**, 969 (1993).
[17] L. S. Schulman, *Techniques and Applications of Path Integration* (Wiley, New York, 1986).
[18] J. S. Langer, Ann. Phys. **41**, 108 (1967).
[19] W. H. Miller, J. Chem. Phys. **62**, 1899 (1975).
[20] S. Coleman, in *The Ways of Subnuclear Physics*, edited by A. Zichichi (Plenum, New York, 1970), p. 805.
[21] I. Affleck, Phys. Rev. Lett. **46**, 388 (1981).
[22] R. F. Dashen, B. Hasslacher, and A. Neveu, Phys. Rev. D **10**, 4114 (1974).
[23] A. O. Caldeira and A. J. Leggett, Ann. Phys. NY **149**, 374 (1983).
[24] F. J. Webster, P. J. Rossky, and R. A. Friesner, Comput. Phys. Commun. **63**, 494 (1991).
[25] J. C. Tully and R. K. Preston, J. Chem. Phys. **55**, 562 (1972).
[26] J. C. Tully, J. Chem. Phys. **93**, 1061 (1990).
[27] D. F. Coker, in *Computer Simulation in Chemical Physics*, edited by M. P. Allen and D. J. Tildesley (Kluwer Academic, The Netherlands, 1993).
[28] P. Pechukas, Phys. Rev. **181**, 166 (1969).
[29] P. Pechukas, Phys. Rev. **181**, 174 (1969).
[30] R. P. Feynman and A. R. Hibbs, *Quantum Mechanics and Path Integrals* (McGraw–Hill, New York, 1965).

[31] R. P. Feynman, *Statistical Mechanics* (Addison–Wesley, Massachusetts, 1972), Chap. 3.
[32] L. Chang and S. Chakravarty, Phys. Rev. B **29**, 130 (1984).
[33] Y. I. Dakhnovskii, A. A. Ovchinnikov, and M. B. Semenov, Mol. Phys. **63**, 497 (1988).
[34] H. Grabert, U. Weiss, and P. Hanggi, Phys. Rev. Lett. **52**, 2193 (1984).
[35] V. A. Benderskii, V. I. Goldanskii, and D. E. Makarov, Chem. Phys. Lett. **171**, 91 (1990).
[36] V. A. Benderskii, V. I. Goldanskii, and D. E. Makarov, Chem. Phys. **154**, 407 (1991).
[37] V. A. Benderskii (unpublished).
[38] P. G. Wolynes, J. Chem. Phys. **87**, 6559 (1987).
[39] D. Chandler, in *Liquides, Cristallisation et Transition Vitreuse Les Houches, Session LI*, edited by D. Levesque, J. Hansen, and J. Zinn-Justin (Elsevier, New York, 1991).
[40] P. Hanggi, P. Talkner, and M. Borkovec, Rev. Mod. Phys. **62**, 250 (1990).